LHC-B 97-007
TRIG

STUDY OF THE LHC-B MUON TRIGGER

M.Borkovsky, A.Tsaregorodtsev, A.Vorobyov

Abstract

This note presents the study of the physics potential of the LHC-B detector with respect to the high-P_t muon trigger. The track finding procedure and requirements to the choice of Fields of Interest are described. Results on the Muon trigger efficiency and geomerical acceptance are presented. Some optimization possibilities are discussed.

Introduction

The goal of this study was to investigate the efficiency of the Muon Trigger that could be provided using the detection planes of the Muon System.

The Muon System was considered as described in the LOI and implemented in the standard SICB package. It includes five detection planes ($\mu 1$ to $\mu 5$), one of which ($\mu 1$) is positioned in front of the electromagnetic calorimeter (Fig.1). We assume that all five detection planes of the Muon System consist of pads with the sizes depending on Z-position of the plane and on the Θ-angle of the pad. The whole Θ-range (10 mr - 300 mr) in each plane is divided into 8 concentric regions, and the pad sizes are determined individually for each such region.

The analysis was performed with the "realistic" magnetic field map in the LHC-B magnet according to the design by PSI.

The event simulation was done with the SICB package which generates minimum bias events as well as $B \rightarrow \mu + X$ events and propagates those events in the LHC-B detector with a full GEANT simulation including interactions of the particles in the material of the detector. The tracks are followed till the energy of the particles is degraded down to the threshold values.

The recent strategy of the LHC-B trigger requires for the Level0 Muon Trigger to provide $\leq 3\%$ retention of the minimum bias events maintaining maximum detection efficiency for the $B \rightarrow \mu + X$ events. Note, that we define the $B \rightarrow \mu + X$ efficiency as the absolute number of the $B \rightarrow \mu + X$ events accepted by the muon trigger related to the total number of the $B \rightarrow \mu + X$ events generated over 4π. Moreover, we require that the triggering muon is the actual muon from direct $B \rightarrow \mu$ decay.

The Level0 muon trigger includes a P_t cut. In the main option, we determine P_t using X-coordinates of the track in $\mu 1$ and $\mu 2$. Also, we investigated an option where the Level0 muon trigger is provided without information from the $\mu 1$ plane operating in severe background conditions. Unfortunately, the efficiency of this trigger proved to be somewhat lower.

Track finding procedure

The track finding starts from a hit in $\mu 3$. Then Fields of Interest (FOI) are determined in $\mu 1, \mu 2, \mu 4, \mu$ 5. The centers of the FOIs in $\mu 2, \mu 4, \mu 5$ are defined along the line drawn through the interaction point and the X,Y-coordinates of the hit in $\mu 3$ defined as the center of the fired pad. The procedure for $\mu 1$ is different. The FOI center in the Y-plane of $\mu 1$ is defined by the line crossing the interaction point and the Y-coordinate of the hit in $\mu 2$ (in fact, this replacement of $\mu 3$ by $\mu 2$ is not important and can be abandoned later). More essential is the way of finding the FOI center in the X-plane of $\mu 1$ by extrapolation of the line defined by the X-coordinates of the hits in $\mu 3$ and $\mu 2$. This extrapolation resolves the muon sign ambiguity and therefore reduces the size of the FOI in $\mu 1$. The sizes of the FOIs depend on Coulomb scattering in iron and on the spatial resolution of the chambers. In addition, one should take into account the spread in the X-planes of $\mu 2, \mu 3, \mu 4$ due to uncertainty in the muon charge sign. The track is accepted if its X,Y-coordinates proved to be inside the FOI of a given plane.

Nominal Fields of Interest

As the first step, we have determined the size of the Nominal Fields of Interest assuming infinitely good spatial resolution. For this purpose 50000 $B \rightarrow \mu + X$ events have been analyzed. The muons with $P_t \geq 1.0$ GeV/c were selected, and the X and Y distributions around the FOI centers were generated in the planes $\mu 1, \mu 2, \mu 4, \mu 5$. Then Δ_x and Δ_y in each plane were found by the condition that 97% of the muons were inside the interval $-\Delta_x \leq$ X-$X_c \leq +\Delta_x$, and similarly 97% of the muons were inside $-\Delta_y \leq$ Y-$Y_c \leq +\Delta_y$. Here X_c, Y_c are the coordinates of the FOI centers. Thus found Δ_x and Δ_y are presented in Tables 1 and 2. Note the difference between Δ_x and Δ_y in $\mu 2, \mu 4, \mu 5$ which is due to the muon sign ambiguity. On the other hand, the larger size of Δ_x in $\mu 1$ is determined by the uncertainty in the extrapolation from $\mu 3, \mu 2$, though the muon sign ambiguity is resolved by such extrapolation.

Θ-range	Δ_x, cm				
mr	$\mu 1$	$\mu 2$	$\mu 3$	$\mu 4$	$\mu 5$
10-20	1.24	1.58	-	1.66	3.41
20-30	2.08	2.33	-	2.50	5.17
30-50	3.29	3.40	-	3.71	7.71
50-100	5.88	5.69	-	6.30	13.16
100-150	9.01	8.42	-	9.40	19.79
150-200	11.47	10.53	-	11.82	25.06
200-250	13.24	12.00	-	13.54	26.97
250-300	14.35	12.85	-	14.57	31.52

Table 1: Nominal fields of interest in X-plane

Fig.2 shows the Θ-dependence of Δ_x and Δ_y. This dependence proved to be not exactly linear, especially in the X planes. The results of the parabolic fits $\Delta_{x,y}\Theta = a_{x,y}\Theta + b_{x,y}\Theta^2$ are presented in Table 3.

Θ-range	Δ_y, cm				
mr	$\mu 1$	$\mu 2$	$\mu 3$	$\mu 4$	$\mu 5$
10-20	0.75	0.61	-	0.76	1.65
20-30	1.13	0.98	-	1.27	2.74
30-50	1.62	1.52	-	2.01	4.35
50-100	2.76	2.69	-	3.61	7.88
100-150	3.98	4.19	-	5.61	12.43
150-200	5.28	5.48	-	7.27	16.41
200-250	6.72	6.55	-	8.59	19.81
250-300	8.00	7.42	-	9.57	22.63

Table 2: Nominal fields of interest in Y-plane

	$\mu 1$	$\mu 2$	$\mu 4$	$\mu 5$
a_x, cm.rad^{-1}	89.3	87.3	96.3	197.8
b_x, cm.rad^{-2}	-135.3	-149.5	-159.2	-315.5
a_y, cm.rad^{-1}	36.85	39.62	53.77	114.9
b_y, cm.rad^{-2}	-30.12	-46.38	-69.21	-119.2

Table 3: Parametrization of nominal FOI width with $\Delta_{x,y} = a_{x,y}\Theta + b_{x,y}\Theta^2$

Pad sizes and FOI sizes

The sizes of the nominal FOIs determine the highest reasonable spatial resolution and the minimal pad sizes in the detection planes. Here we define the pad sizes as

$$d_x(\mu i) = K_x(\mu i)\Delta_x(\mu i), \qquad d_y(\mu i) = K_y(\mu i)\Delta_y(\mu i) \tag{1}$$

where $d_{x,y}$ are the full widths of the pads, and $K_{x,y}$ are some variable coefficients. For example:

$K_{x,y} = 0.02$ — very high resolution,

$K_{x,y} = 0.2$ — high resolution,

$K_{x,y} = 0.5$ — nominal resolution.

In our analysis, the pad sizes $d_{x,y}$ were constant inside each of the Θ-ranges shown in Table 1, and the coefficients $K_{x,y}$ were independent on the Θ-range. Note that defining $d_{x,y}$ in $\mu 3$ we used eq.(1) with $\Delta_{x,y}(\mu 3) \equiv \Delta_{x,y}(\mu 2)$.

As an example, in case of nominal resolution ($K_{x,y} = 0.5$) the pad sizes in $\mu 2(\mu 3)$ varied from $d_x = 8$ mm, $d_y = 3$ mm in the Θ-range (10–20) mr to $d_x = 64$ mm, $d_y = 37$ mm in the Θ-range (250–300) mr.

Following the track finding procedure described above, the hits should be found first in $\mu 3$ and then in the fields of interest in $\mu 4, \mu 5, \mu 2$, and $\mu 1$. The sizes of these FOIs we define as

$$D_x(\mu i) = C_x(\mu i)\Delta_x(\mu i), \qquad D_y(\mu i) = C_y(\mu i)\Delta_y(\mu i) \tag{2}$$

where $C_{x,y}$ are variable coefficients independent on the Θ-range. The values of $D_{x,y}$ are constant inside each Θ-range shown in Table 1. The track is accepted if its X,Y-coordinates, defined as the center of the fired pad, proved to be within $\pm D_{x,y}$ around the center of the FOI. In most part of our analysis we used $K_{x,y} = 0.5$ in all planes (except $K_y(\mu 1) = 1$), while the coefficients $C_{x,y}$ were varied to optimize the muon trigger.

Track finding efficiency

The results presented below are based on analysis of 5000 MB events and 7000 $B \to \mu + X$ events. Fig.3 shows how the $B \to \mu + X$ efficiency and MB retention depend on the sizes of the fields of interest. Fig.3a corresponds to the case when the FOI sizes were varied simultaneously in $\mu 2$, $\mu 4$, and $\mu 5$ while the FOI in $\mu 1$ was kept widely open ($C_{x,y} = 15$). One of the curves ($P_t \geq 0.02$ GeV/c) represents all detected muons, the other one - the muons with $P_t \geq 1.0$ GeV/c. One can see the saturation effect with increase of C_{var} especially in the case of $P_t \geq 1.0$ GeV/c. From this figure it follows that the maximum $B \to \mu + X$ detection efficiency provided by

the Muon System is 18% ($P_t \geq 0.02$ GeV/c) and 14% ($P_t \geq 1.0$ GeV/c). The opening of the FOIs leads to fast increase of the MB retention. So it is desirable that the values of $C_{x,y}(\mu 2), C_{x,y}(\mu 4), C_{x,y}(\mu 5)$ would not exceed $C_i \cong 1.2$. Fig.3b shows similar curves for the case where FOIs were varied simultaneously in all planes ($\mu 1, \mu 2, \mu 4, \mu 5$). One can see that inclusion of $\mu 1$ shifted the saturation region to $C_i \geq 1.5$, the saturated values for $B \rightarrow \mu + X$ efficiency being on the same level as without $\mu 1$.

Muon trigger

The muon trigger includes the described above track finding followed by the P_t cut. The schematic of the trigger is as follows.

1. Finding a hit in $\mu 3$. The hit X,Y-coordinates are the X_c, Y_c coordinates of the center of the fired pad.
2. Finding X- and Y-coordinates of the FOIs centers in $\mu 2, \mu 4, \mu 5$.
3. Finding hits in $\mu 2, \mu 4, \mu 5$ in the corresponding FOIs. In case the number of hits exceeds 1, we take the hit nearest to the center of the FOI.
4. Finding Y- and X-coordinates of the FOI center in $\mu 1$.
5. Finding hits in the FOI in $\mu 1$. In case the number of hits exceed 1, we take the hit nearest to the center of the FOI.
6. Calculating P_t using X-coordinates of the track in $\mu 1$ and $\mu 2$. Applying the appropriate P_t cut.

Now we should make one remark concerning the occupancy in $\mu 1$. Even with the smallest possible FOIs in $\mu 1$ the occupancy of these FOIs may be 20% or more. As it was mentioned above, in case of more than 1 hit in the FOI we take the nearest one to the center of the FOI. This logic takes advantage of the fact that the accidental hits are distributed uniformly in the FOI while the correct track distribution is concentrated around the FOI center. This enhances essentially the probability to find the correct track. Still some probability remains that the hit from the searched track is substituted by the accidental one. What is the consequence of such substitution for the P_t cut? One can see that in this case P_t will be actually measured not by the X-coordinates in $\mu 1$ and $\mu 2$ but by the X-coordinates in $\mu 2$ and $\mu 3$. Though this measurement is less precise, still it provides reasonable trigger efficiency as it will be shown below. So the described trigger logic can work satisfactory at quite large occupancies.

Muon trigger optimization

In the following we determined the $B \rightarrow \mu + X$ efficiency and minimum bias retention under various conditions.

- The pad sizes were fixed: all $K_i = 0.5$ except $K_y(\mu 1) = 1.0$.
- The fields of interest (C_i) could be varied independently in each plane.

	3% MB retention		1% MB retention	
C_i	$B \to \mu$ eff.%	P_t cut, GeV/c	$B \to \mu$ eff.%	P_t cut, GeV/c
1.0	11.5	0.5	8.3	1.4
1.2	12.8	0.7	8.7	1.5
1.5	13.5	0.8	8.7	1.7
2.0	13.1	1.0	7.5	1.9
2.0/1.2	13.4	1.0	8.5	1.7

Table 4: $B \to \mu$ efficiencies at $\mu1/\mu2$ P_t cuts corresponding to 3% and 1% MB retention

- For a given set of C_i, the P_t cut was varied from $P_t = 0.02$ GeV/c to $P_t = 3.0$ GeV/c.
- Two options for pt determination were considered: using extrapolations from $\mu1/\mu2$ or from $\mu2/\mu3$.

Figs.4 and 5 present the $B \to \mu + X$ efficiency vs. MB retention plots for several sets of C_i:
$C_{x,y}(\mu1) = C_{x,y}(\mu2) = C_{x,y}(\mu4) = C_{x,y}(\mu5) = 1.0;\ 1.2;\ 1.5;\ 2.0;$
$C_{x,y}(\mu1) = 1.5;\ 2.0;$
$C_{x,y}(\mu2) = C_{x,y}(\mu4) = C_{x,y}(\mu5) = 1.2.$
The corresponding dependencies of the $B \to \mu + X$ efficiencies on the P_t cut are shown in Figs.6 and 7. We see that with the appropriate $\mu1/\mu2$ P_t cuts one can obtain the $B \to \mu + X$ efficiency of 13% at the 3% MB retention level and around 9% at 1% MB retention (Table 4). The optimal values of the C_i coefficients seem to be around 1.5.

Figs.8 and 9 show the trigger efficiency with $\mu2/\mu3$ P_t cut in comparison with $\mu1/\mu2$ P_t cut. One can see that substitution of the correct hit in the $\mu1$ FOI by an accidental one leading to substitution of the $\mu1/\mu2$ P_t cut by the $\mu2/\mu3$ P_t cut does not change much the trigger quality. Our analysis showed that the accidental hits in $\mu1$ were accepted instead of correct hits in 16% of the tracks used for P_t cut. This value was obtained with $C_{x,y}(\mu1)$=2, and it was averaged over the whole Θ-range. In fact, the probability is much higher ($\approx$ 25%) in the zone between 50 mr to 150 mr, and it is negligible at $\Theta \geq 200$ mr. Note also that the real occupancy in $\mu1$ might be considerably higher than in the present analysis. Similar probability for $\mu2$ was found to be much smaller (1.3%).

A natural question arises if one can provide the Level0 muon trigger not using the $\mu1$ at all. This would simplify considerably the trigger logic. Note that the data in Figs.8 and 9 corresponding to the $\mu2/\mu3$ P_t cut are obtained with requirement of a hit in the $\mu1$ FOI. With this requirement, one can obtain the $\mu2/\mu3$ trigger efficiency on a level of 11.5% at 3% MB retention.

Fig.10 presents the results of the analysis without using information from $\mu1$. One can see that in this option it is also possible to obtain 11.5% $B \to \mu + X$ efficiency at the 3% MB retention with reduced FOIs:

$$C_{x,y}(\mu2) = C_{x,y}(\mu4) = C_{x,y}(\mu5) = 0.8.$$

The 3% MB retention is obtained with the $\mu2/\mu3$ P_t cut around 1.0 GeV/c. The conclusion is that the Level0 muon trigger can be provided without the $\mu1$ plane, however, the $B \to \mu + X$ efficiency will be decreased by 15%.

Zone,	Θ-range,	$B \to \mu + X$ tracks		Min.Bias tracks	
#	mr	$P_t \geq 0.02$ GeV/c	$P_t \geq 0.8$ GeV/c	$P_t \geq 0.02$ GeV/c	$P_t \geq 0.8$ GeV/c
1	10–20	1.66	1.53	0.69	0.15
2	20–30	1.54	1.31	0.97	0.15
3	30–50	2.51	2.16	2.01	0.32
4	50–100	4.41	3.51	5.54	1.08
5	100–150	2.61	2.16	3.26	0.7
6	150–200	2.49	2.13	1.39	0.48
7	200–250	1.27	1.19	0.38	0.20
8	250–300	0.91	0.87	0.14	0.13
9	>300	0.26	0.26	0.06	0.06
	Total	17.87	15.11	14.4	3.27

Table 5: Number of μ-tracks from $B \to \mu$ decays and number of MB tracks per 100 $B \to \mu$ and 100 MB events, respectively, for $\mu 1/\mu 2$ P_t = 0.02 GeV/c; 0.8 GeV/c

Further study will show if this efficiency could be improved by applying some other cuts, for example, by rejection large scattering angles measured by $\mu 4$ and $\mu 5$. At this moment, we consider the $\mu 1/\mu 2$ P_t trigger with $C_i \cong 1.5$ as the main option.

Geometrical acceptance

The Θ-distributions of the μ-tracks from the $B \to \mu + X$ decays as well as the MB tracks selected by the track finding procedure are presented in Table 5 and shown in Fig.11. The FOIs in the muon planes were

$$C_{x,y}(\mu 1) = C_{x,y}(\mu 2) = C_{x,y}(\mu 4) = C_{x,y}(\mu 5) = 1.5.$$

The distributions are shown before and after the $\mu 1/\mu 2$ P_t cut. Presented are the numbers of the μ-tracks from $B \to \mu + X$ decays per 100 $B \to \mu + X$ decays and the numbers of MB tracks per 100 MB events.

Some conclusions from these distributions:

- The Θ-zones from 10–50 mr, 50–150 mr, and >150 mr contributes approximately equally to the μ-trigger rate.
- The MB-tracks are more concentrated in the 50–150 mr zone, while the background at $\Theta > 200$ mr is much smaller.
- The P_t cut kills uniformly the good μ-tracks at $\Theta < 200$ mr and less at larger angles that could be the consequence of absorption of low P_t tracks in iron.

Fig.12 illustrate dependence of the trigger rate on Θ_{max} and Θ_{min}.

One can see that reduction of Θ_{max} from 300 mr to 250, 200, 150 mr decreases the trigger rate by 6%, 14%, and 30%, respectively. Similarly, the increase of Θ_{min} from 10 mr to 20 mr and 30 mr decreases the trigger rate by 10% and 18%, respectively. Taking into account relatively low background at $\Theta > 200$ mr, this large angle Θ-range looks attractive. Fig.13

shows that dependence of the trigger efficiency on Θ_{max} and Θ_{min} is not sensitive to the P_t cut. Similar conclusion can be done on the MB retention (Figs.14 and 15).

Conclusion

The following conclusions can be drawn from the presented analysis.

- The muon system can provide the Level0 trigger in the stand-alone mode, i.e. without using information from the tracking stations. With $\mu 2/\mu 1$ P_t cut mode, the 3% Minimum Bias retention is obtained at P_t cut = 0.8 GeV/c thus providing 13.5% $B \rightarrow \mu + X$ efficiency (compare with the total $B \rightarrow \mu + X$ efficiency of 18% for $P_t \geq 0.02$ GeV/c and 14% for $P_t \geq 1.0$ GeV/c). The 1% retention can be reached with P_t cut = 1.7 GeV/c corresponding to about 9% $B \rightarrow \mu + X$ efficiency.

- The $\mu 2/\mu 1$ P_t cut mode assumes extrapolation in the X-plane of the trajectory measured by $\mu 3/\mu 2$ stations to the $\mu 1$ station. This extrapolation eliminates the muon sign ambiguity and reduces the influence of the occupancy in $\mu 1$ on the efficiency of the muon trigger. On the other hand, this requires precise enough measurements of the X-coordinates in $\mu 1, \mu 2$, and $\mu 3$. The pad sizes in these stations should not exceed $d_x = 0.5\ \Delta_x(\mu i)$ where $\Delta_x(\mu i)$ are the half-widths of the nominal fields-of-interest presented in this report.

- The suggested scheme allows also to use the P_t cut based on the trajectory measurements only in stations $\mu 3/\mu 2$. In this case, the 3% MB retention could be obtained with 11% $B \rightarrow \mu + X$ efficiency. The advantage of this mode is that it does not depend on the occupancy conditions in $\mu 1$. The disadvantage is the 20% loss in the trigger efficiency.

- The study of the muon trigger efficiency dependence on Θ_{min} and Θ_{max} of the muon system showed that the reduction of Θ_{max} from 300 mrad to 250 mrad leads to only 6% decrease in the trigger efficiency. So such reduction could be recommended to reduce the cost of the Muon System.

- The other possibility to reduce the Muon System cost might be to abandon one of the two downstream stations ($\mu 4$), which are used only for muon ID, with redistribution of the muon iron into two blocks (instead of three).

- One could consider also a possibility to use concrete (instead of iron) in the outer region of the muon system.

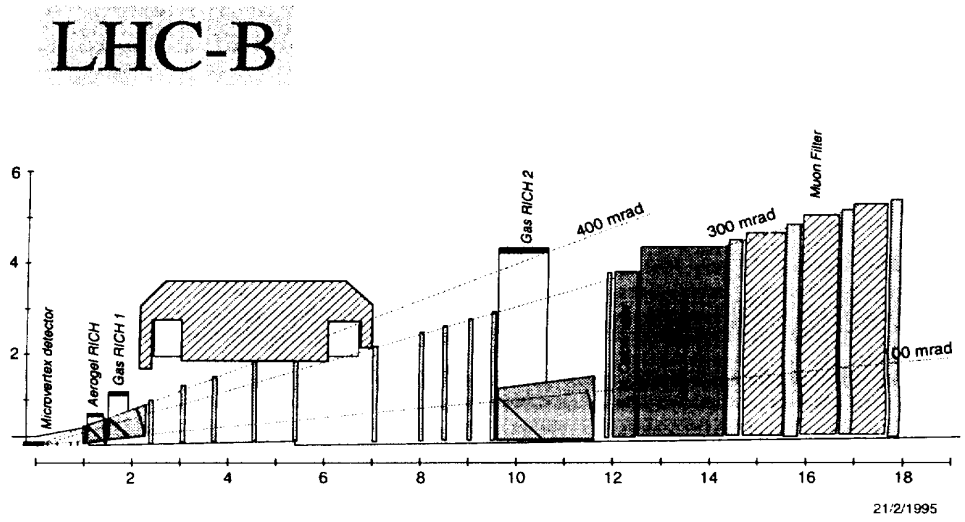

Figure 1: The LHC-B detector general layout
Z-position of the muon chambers :
$\mu 1$ - 11.66m
$\mu 2$ - 14.55m
$\mu 3$ - 15.65m
$\mu 4$ - 16.70m
$\mu 5$ - 17.80m

Nominal Fields of Interest in X-plane

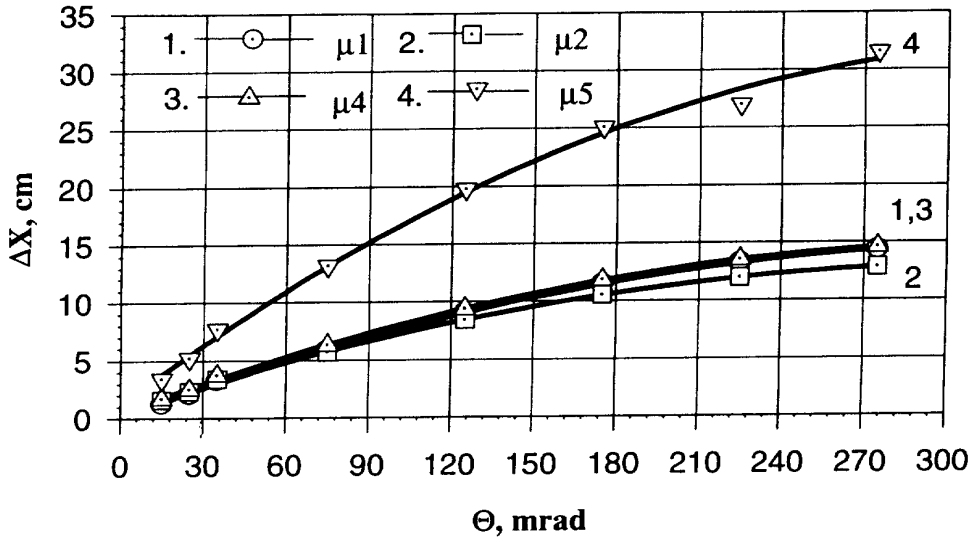

Nominal Fields of Interest in Y-plane

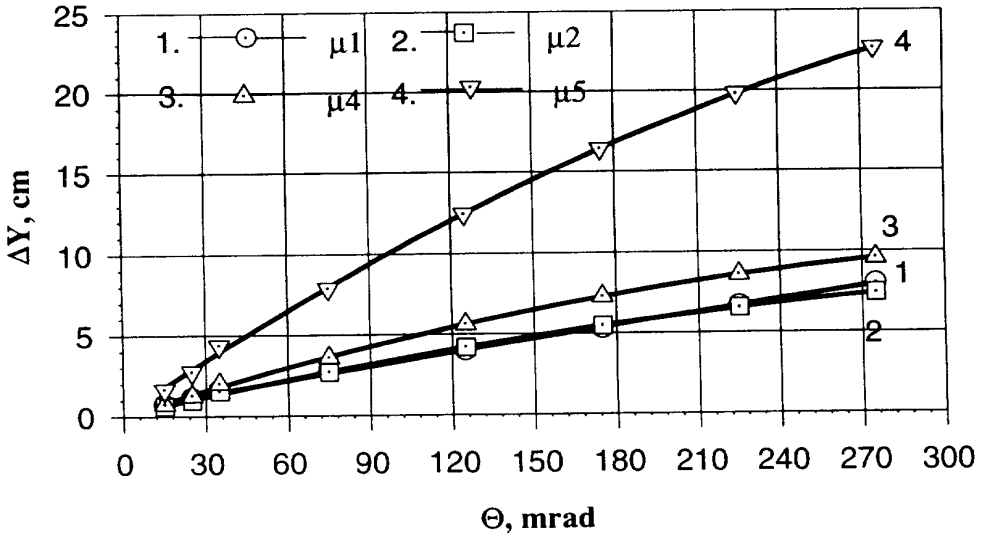

Figure 2: Nominal fields of interest in X & Y-planes

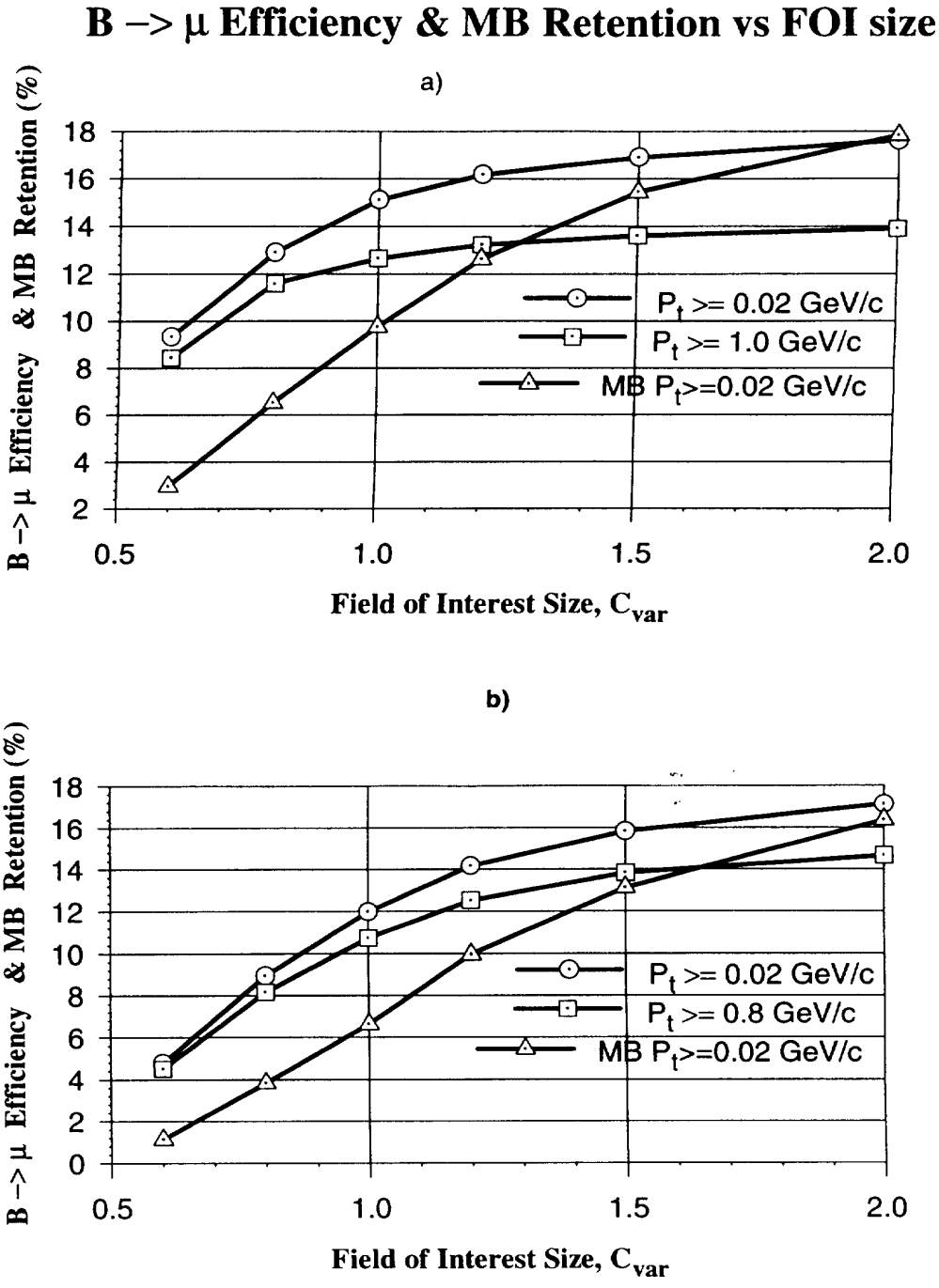

Figure 3: B $\rightarrow \mu$ efficiency & MB retention vs. FOI size.
a) $C_{x,y}(\mu 1) = 1.5$, $C_{x,y}(\mu 2) = C_{x,y}(\mu 4) = C_{x,y}(\mu 5) = C_{var}$
b) $C_{x,y}(\mu 1) = C_{x,y}(\mu 2) = C_{x,y}(\mu 4) = C_{x,y}(\mu 5) = C_{var}$

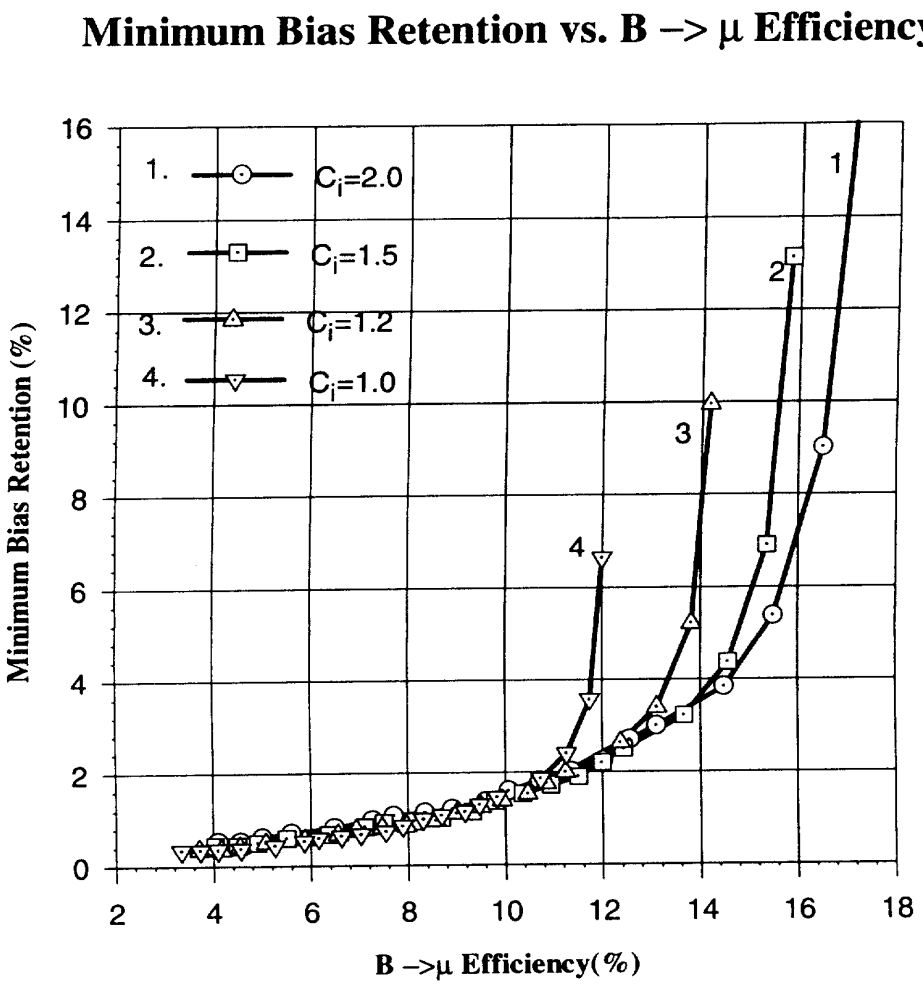

Figure 4: Minimun Bias retention vs. B $\rightarrow \mu$ efficiency. $\mu 1/\mu 2 P_t$ cut. $C_{x,y}(\mu 1) = C_{x,y}(\mu 2) = C_{x,y}(\mu 4) = C_{x,y}(\mu 5)$=1.0; 1.2; 1.5; 2.0

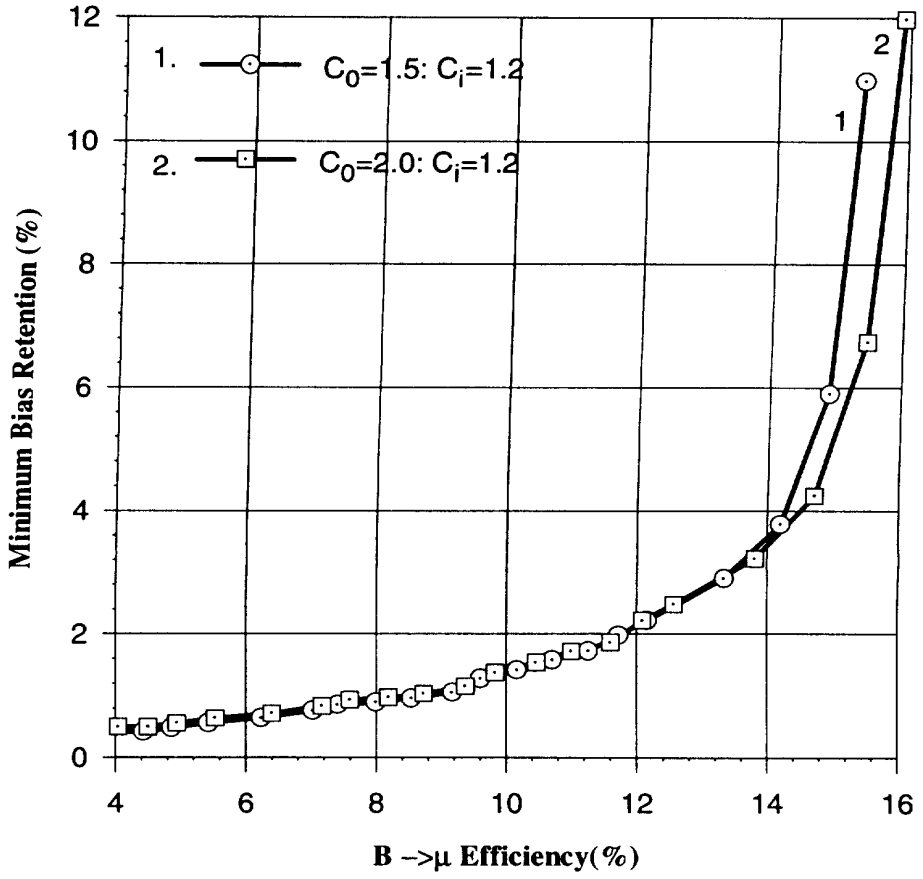

Figure 5: Minimun Bias retention vs. B $\rightarrow \mu$ efficiency. $\mu 2/\mu 1 P_t cut$.
$C_{x,y}(\mu 1)$=1.5; 2.0 ,
$C_{x,y}(\mu 2) = C_{x,y}(\mu 4) = C_{x,y}(\mu 5)$=1.2

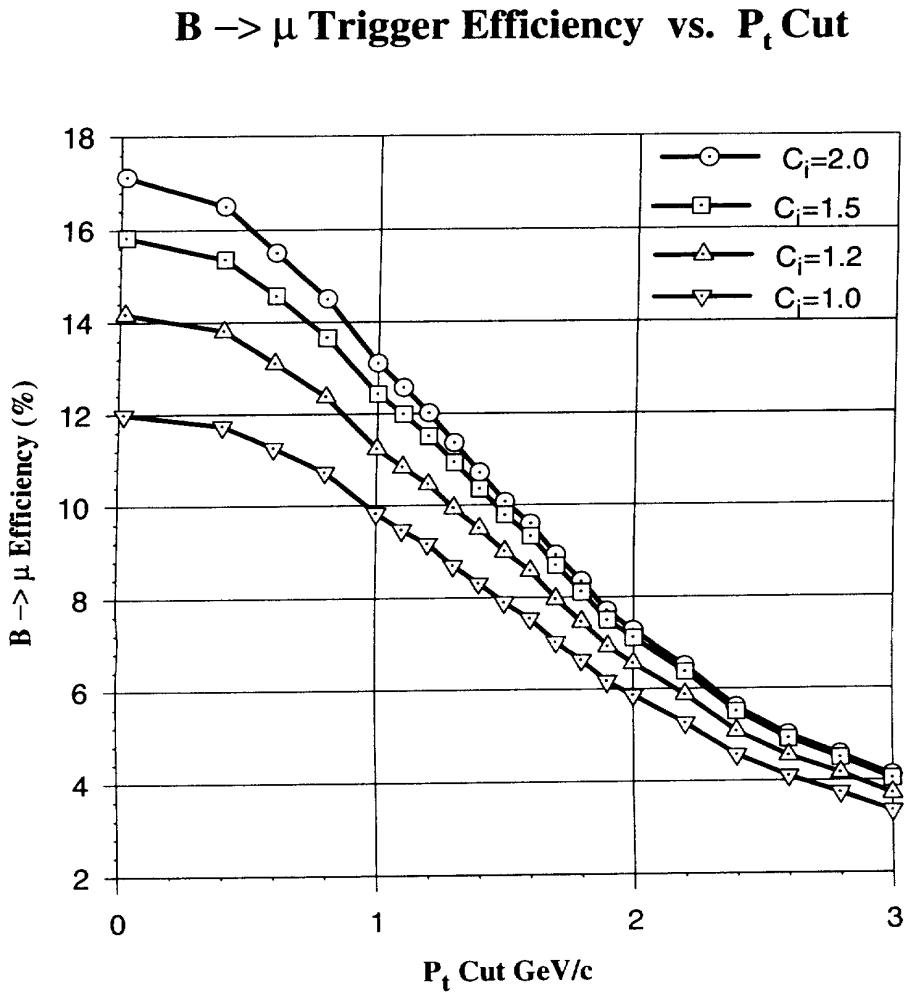

Figure 6: B $\rightarrow \mu$ trigger efficiency vs. $\mu 1/\mu 2 P_t$ cut.
$C_{x,y}(\mu 1) = C_{x,y}(\mu 2) = C_{x,y}(\mu 4) = C_{x,y}(\mu 5)$=1.0; 1.2; 1.5; 2.0

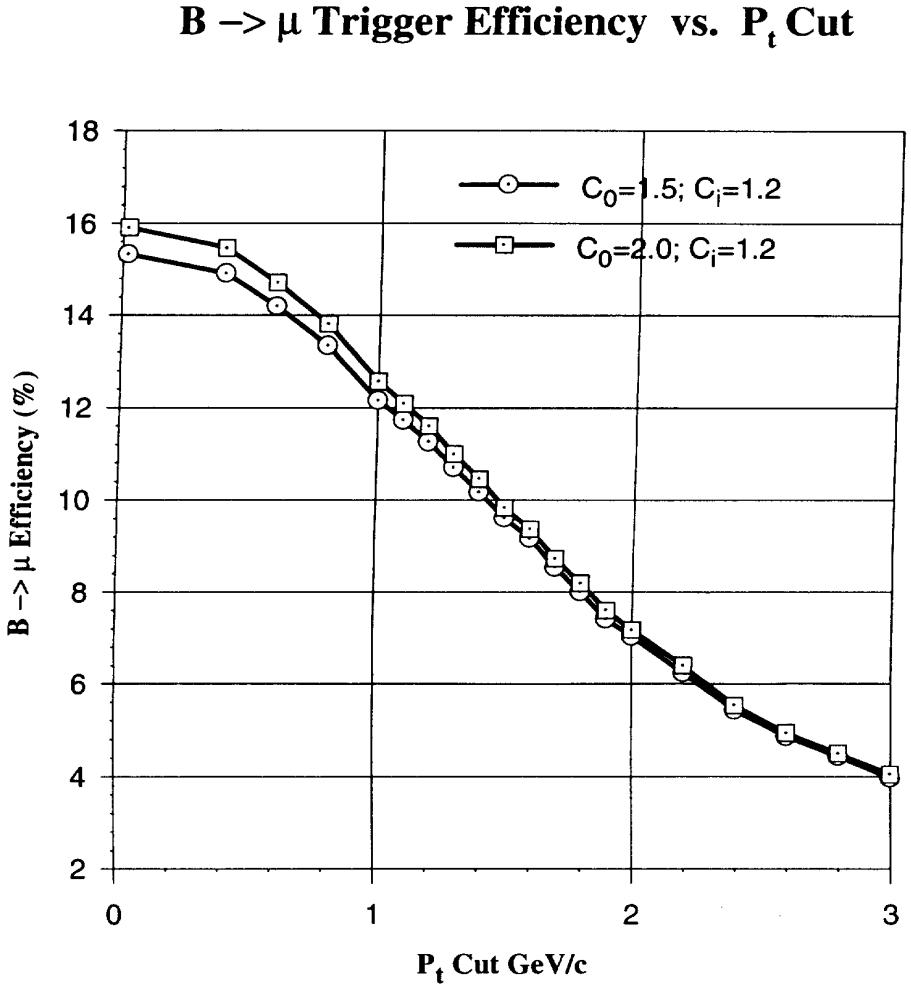

Figure 7: B $\rightarrow \mu$ trigger efficiency vs. $\mu 1/\mu 2 P_t$ cut.
$C_{x,y}(\mu 1)$=1.5; 2.0 ,
$C_{x,y}(\mu 2) = C_{x,y}(\mu 4) = C_{x,y}(\mu 5)$=1.2

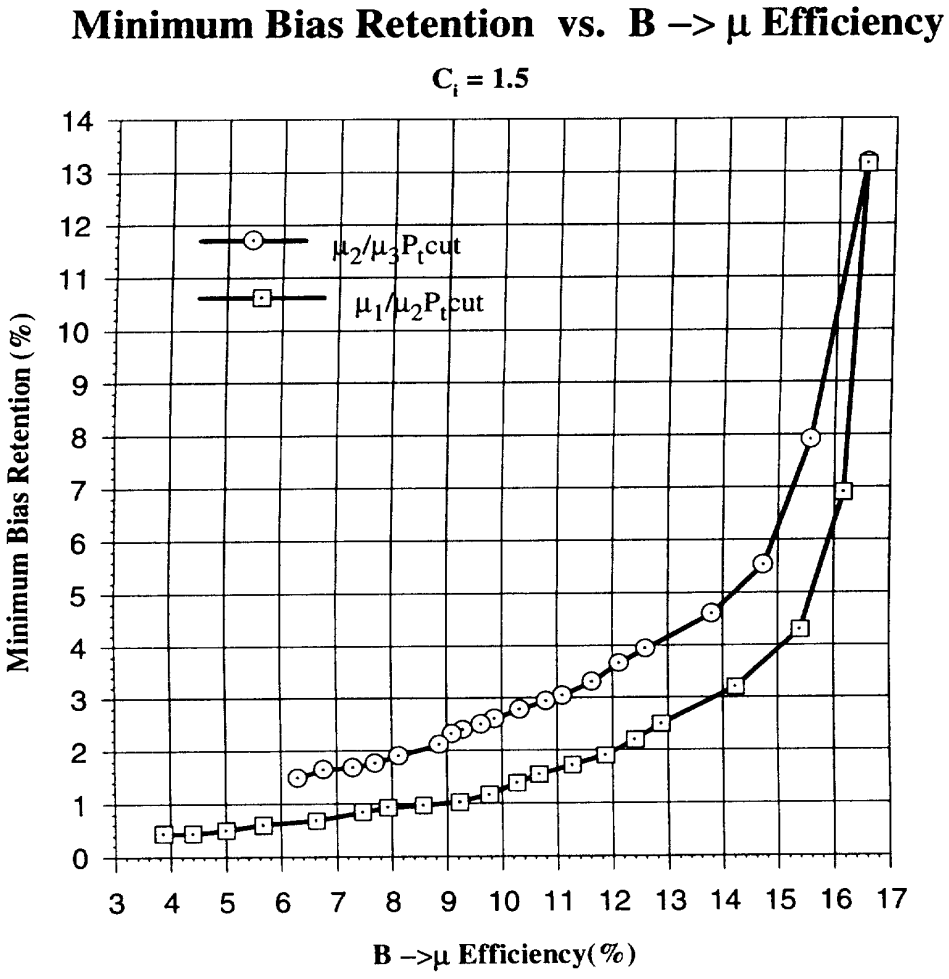

Figure 8: Minimun Bias retention vs. B $\rightarrow \mu$ efficiency.
Comparison of $\mu 2/\mu 3 P_t$ cut with $\mu 1/\mu 2 P_t$ cut.
$C_{x,y}(\mu 1) = C_{x,y}(\mu 2) = C_{x,y}(\mu 4) = C_{x,y}(\mu 5)$=1.5

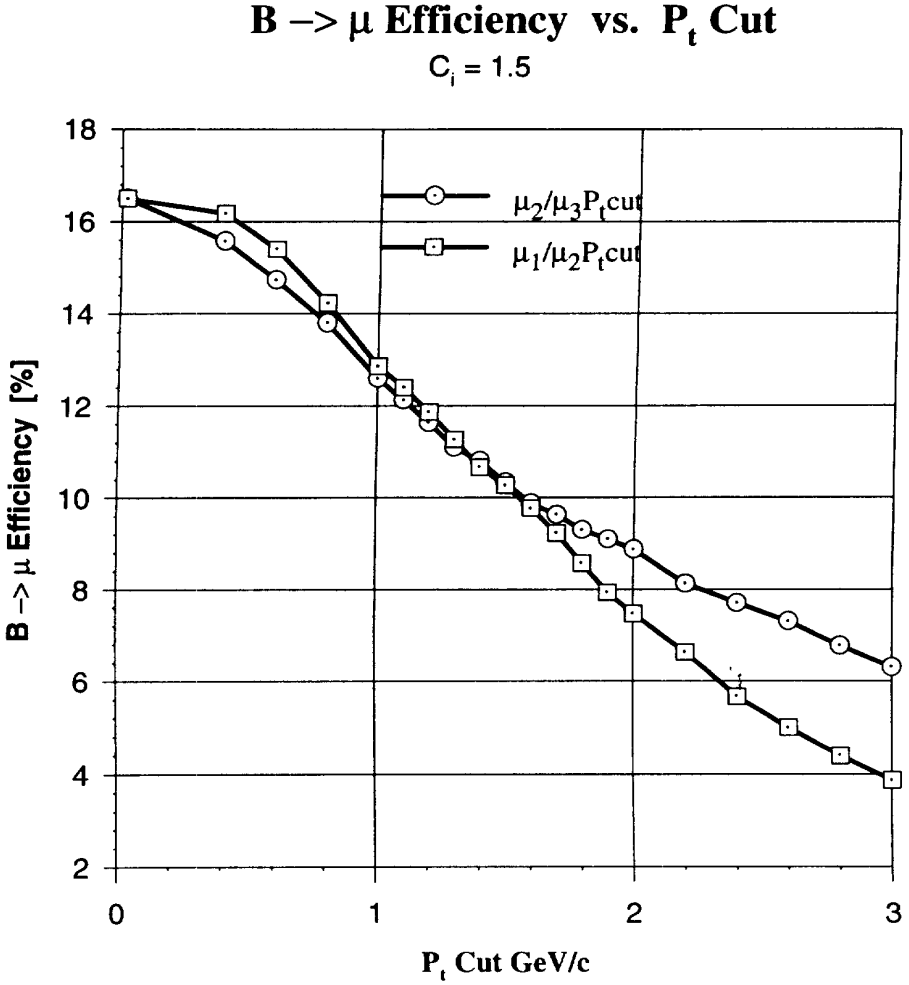

Figure 9: B $\rightarrow \mu$ efficiency vs. P_t cut.
Comparison of $\mu 2/\mu 3 P_t$ cut with $\mu 1/\mu 2 P_t$ cut.
$C_{x,y}(\mu 1) = C_{x,y}(\mu 2) = C_{x,y}(\mu 4) = C_{x,y}(\mu 5)$=1.5

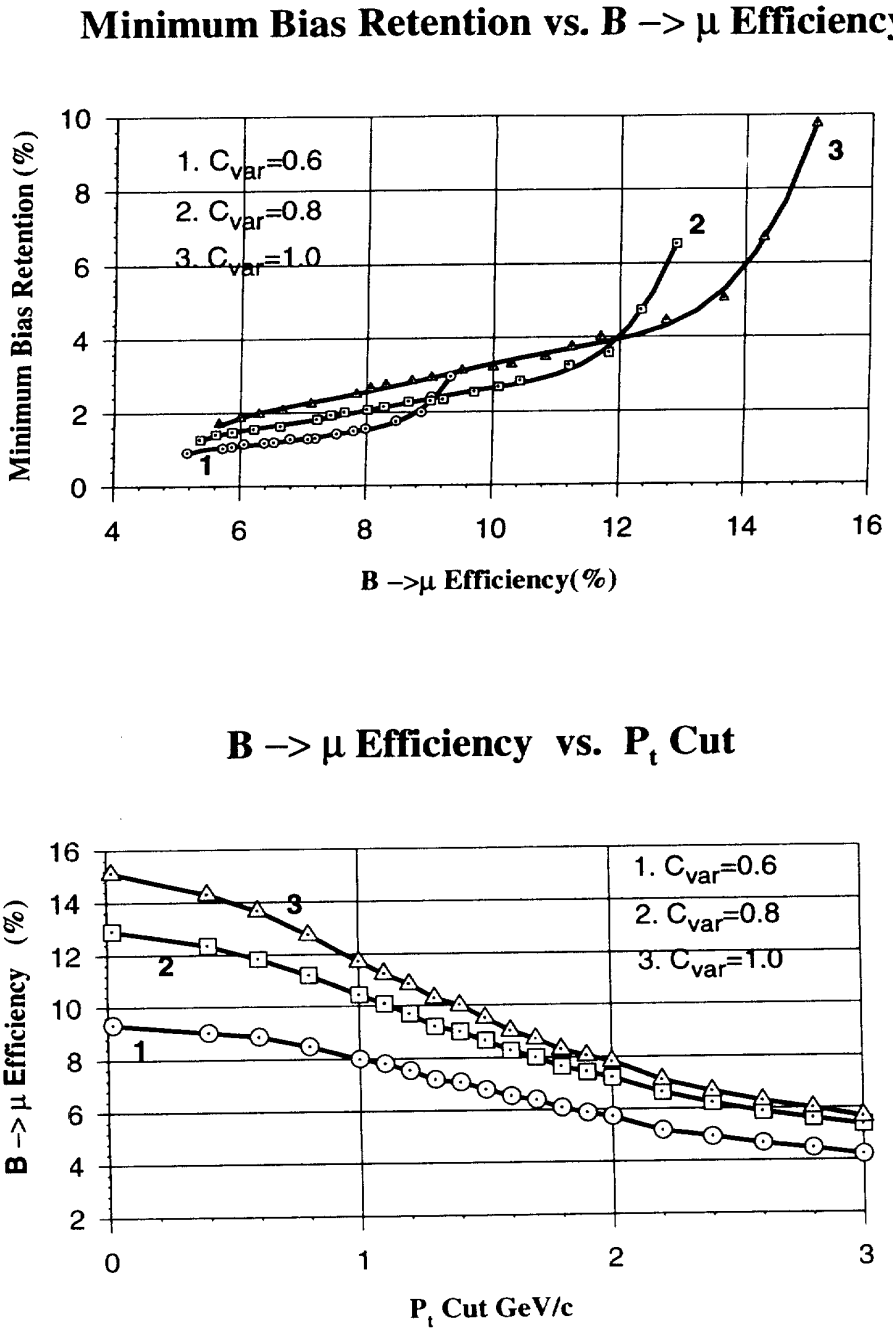

Figure 10: B $\rightarrow \mu$ efficiency & MB retention. $\mu 2/\mu 3 P_t$ cut.
$C_{x,y}(\mu 1)$=15,
$C_{x,y}(\mu 2) = C_{x,y}(\mu 4) = C_{x,y}(\mu 5) = C_{var}$= 0.6; 0.8; 1.0.

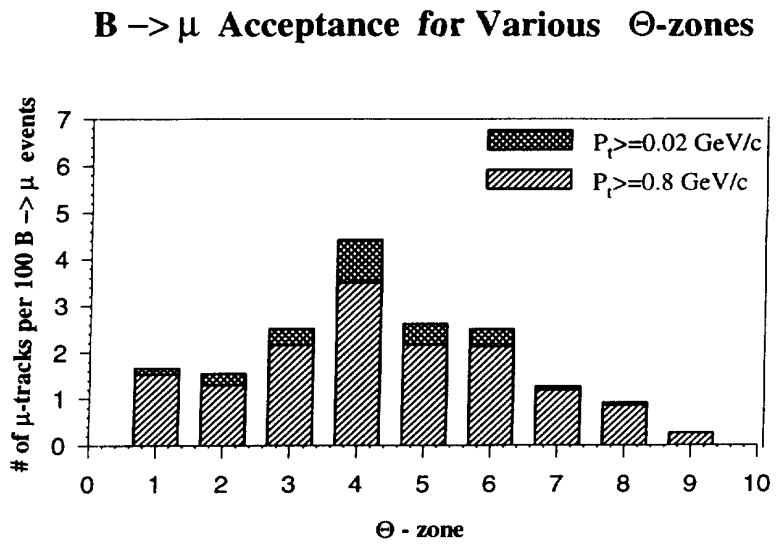

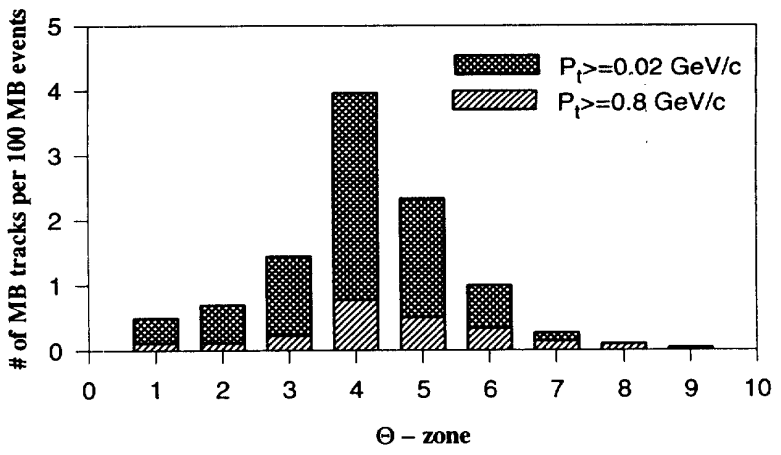

Figure 11: Relative number of accepted B $\rightarrow \mu$ tracks & MB tracks for various Θ-zones.

Θ-zone	1	2	3	4	5	6	7	8	9
Θ mr	10-20	20-30	30-50	50-100	100-150	150-200	200-250	250-300	¿300

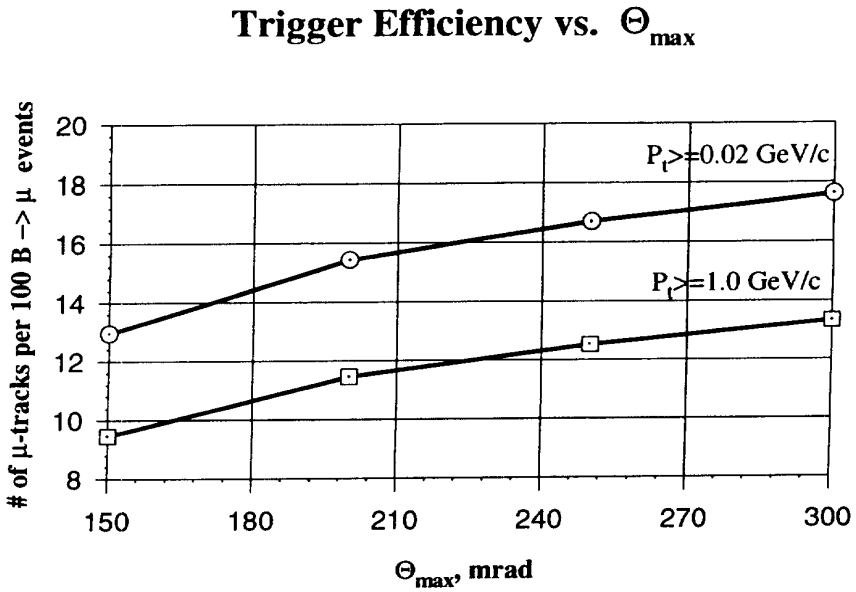

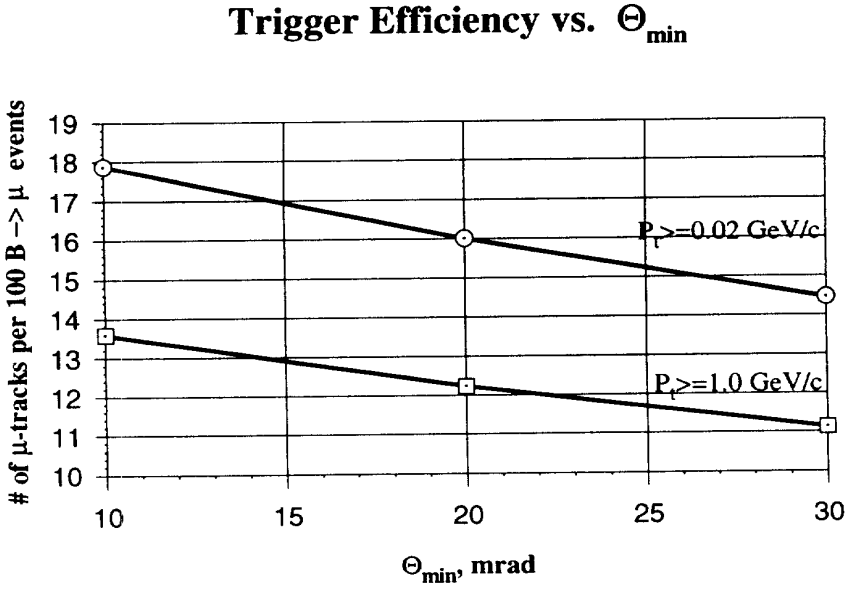

Figure 12: Trigger efficiency vs. Θ_{max}&Θ_{min}
for various $\mu 1/\mu 2 P_t$ cut
$C_{x,y}(\mu 1) = C_{x,y}(\mu 2) = C_{x,y}(\mu 4) = C_{x,y}(\mu 5)$=1.5

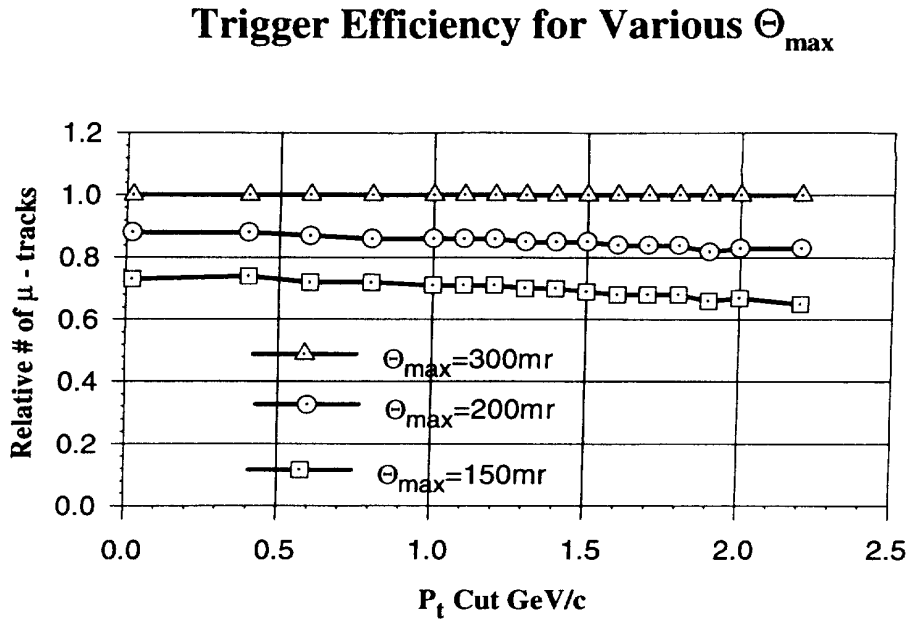

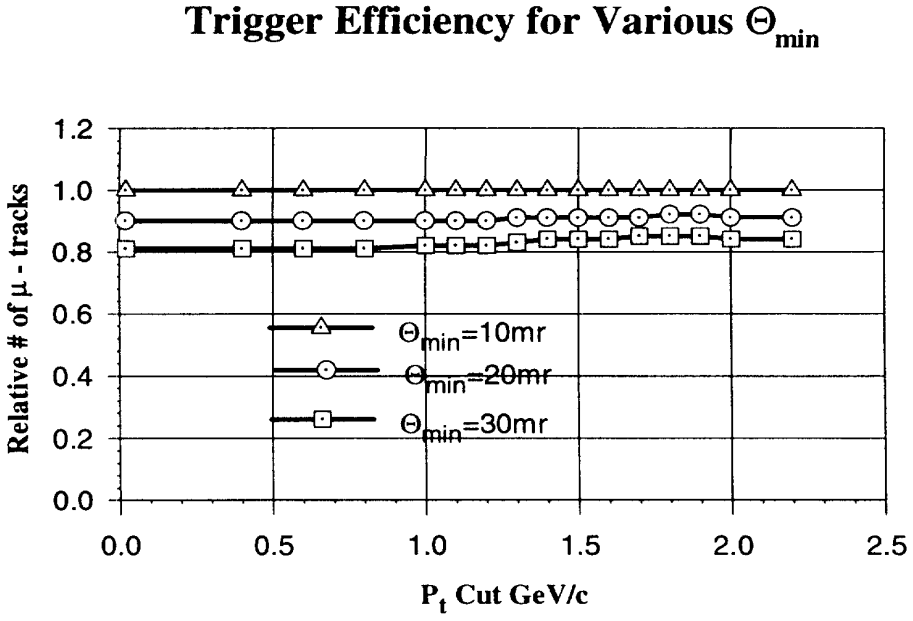

Figure 13: Relative number of accepted μ tracks from
B $\rightarrow \mu$ vs. $\mu 1/\mu 2 P_t$ cut
for various Θ_{max}&Θ_{min}.
$C_{x,y}(\mu 1) = C_{x,y}(\mu 2) = C_{x,y}(\mu 4) = C_{x,y}(\mu 5)$=1.5

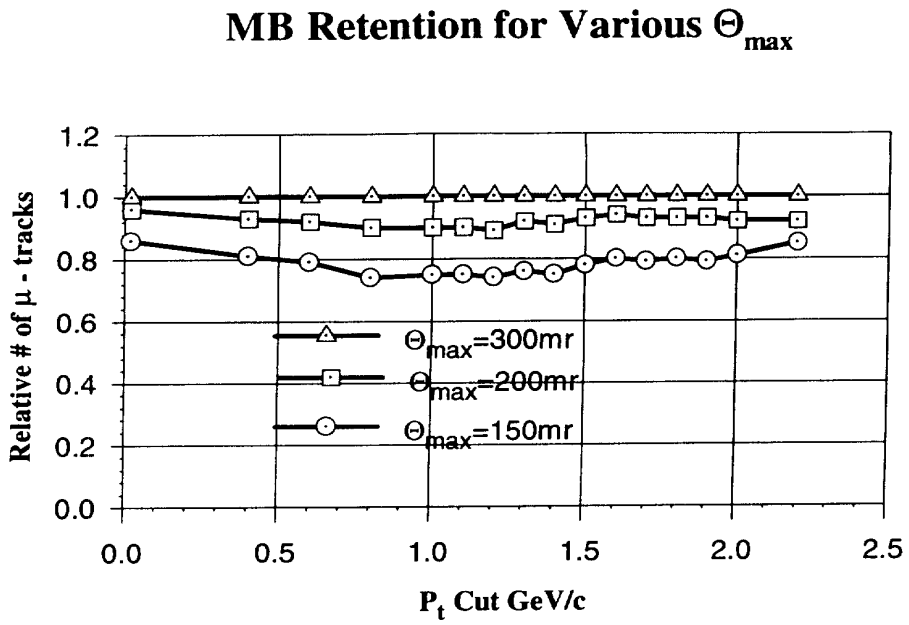

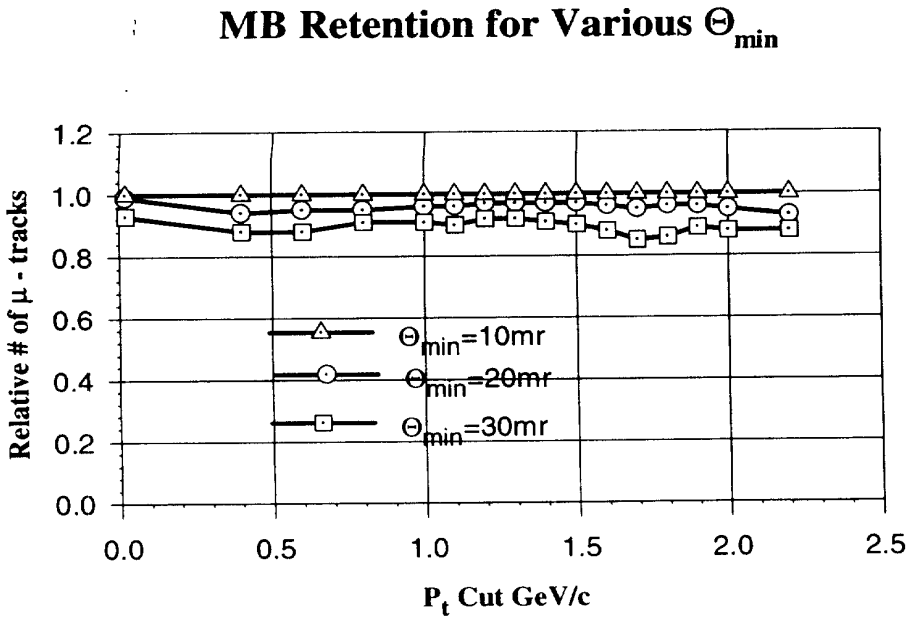

Figure 14: Relative number of accepted MB tracks vs. $\mu 1/\mu 2 P_t$ cut for various Θ_{max}&Θ_{min}.
$C_{x,y}(\mu 1) = C_{x,y}(\mu 2) = C_{x,y}(\mu 4) = C_{x,y}(\mu 5)$=1.5

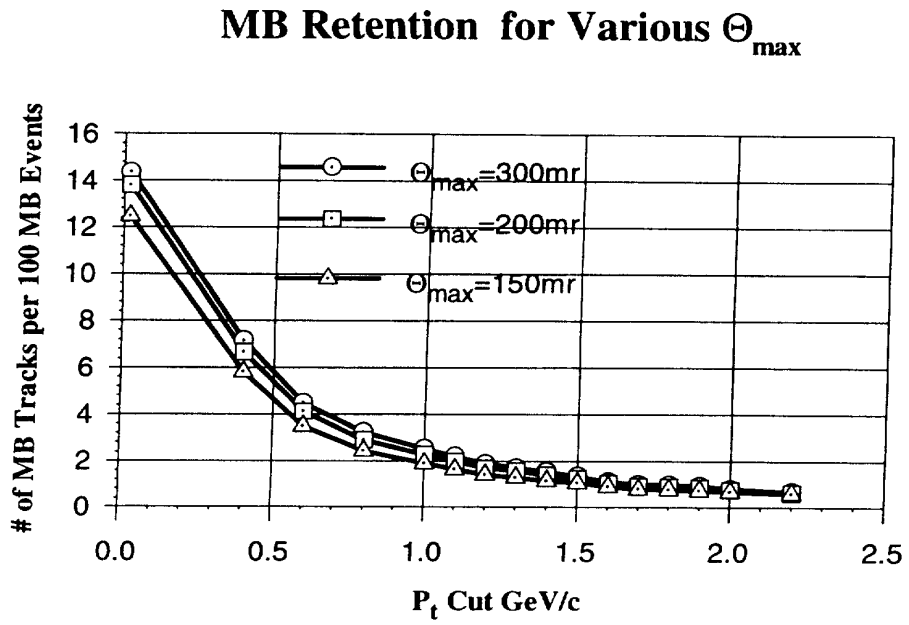

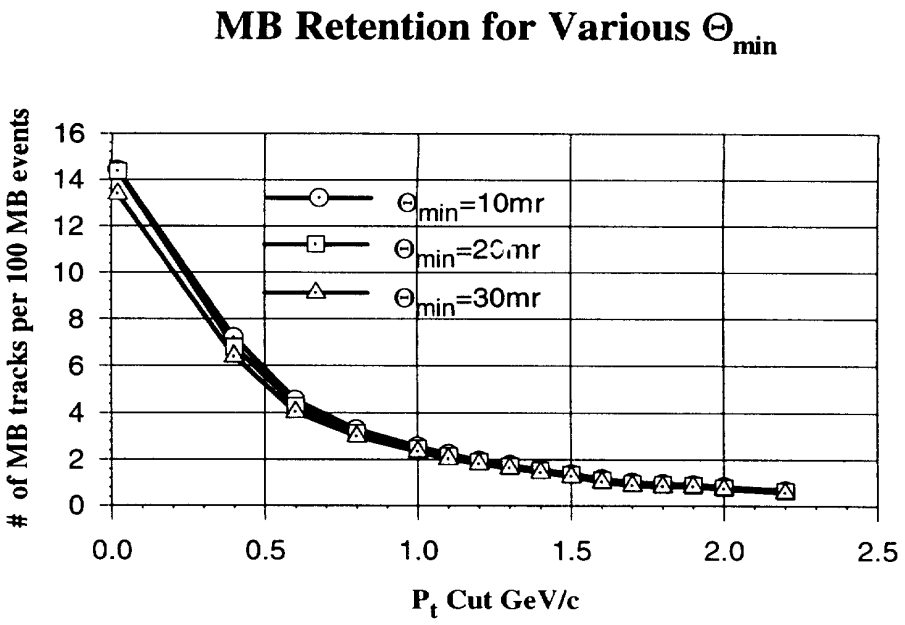

Figure 15: Relative number of accepted MB tracks vs. $\mu 1/\mu 2 P_t$ cut for various Θ_{max}&Θ_{min}.
$C_{x,y}(\mu 1) = C_{x,y}(\mu 2) = C_{x,y}(\mu 4) = C_{x,y}(\mu 5)$=1.5